

K-11

**RI 9407**

**REPORT OF INVESTIGATIONS/1992**

## **Remote Fiber-Optic Methane Monitor**

By T. H. Dubaniewicz, Jr., and J. E. Chilton

**UNITED STATES DEPARTMENT OF THE INTERIOR**



**BUREAU OF MINES**



**Report of Investigations 9407**

**Remote Fiber-Optic Methane Monitor**

**By T. H. Dubaniewicz, Jr., and J. E. Chilton**

**UNITED STATES DEPARTMENT OF THE INTERIOR**  
**Manuel Lujan, Jr., Secretary**

**BUREAU OF MINES**  
**T S Ary, Director**

**Library of Congress Cataloging in Publication Data:**

**Dubaniewicz, T. H. (Thomas H.)**

Remote fiber-optic methane monitor / by T.H. Dubaniewicz, Jr., and J.E. Chilton

p. cm. -- (Report of investigations; 9407)

Includes bibliographical references (p. 8).

Supt. of Docs. no.: I 28.23:9407.

1. Fire-damp--Measurement. 2. Optical detectors--Testing. 3. Fiber optics.  
I. Chilton, J. E. II. Title. III. Series: Report of investigations (United States.  
Bureau of Mines); 9407.

TN23.U43 [TN305] 622 s--dc20 [622'.82] 91-44299 CIP

## CONTENTS

	<i>Page</i>
Abstract .....	1
Introduction .....	2
System components .....	2
Results .....	4
Temperature effects .....	5
Refractive index effects .....	5
Macrobending effects .....	7
Summary .....	7
References .....	8

## ILLUSTRATIONS

1. Profile of fiber-optic cable .....	2
2. Fiber-optic CH <sub>4</sub> monitor .....	3
3. Fiber-optic window and CH <sub>4</sub> absorption peak .....	3
4. Percent power loss for various concentrations of CH <sub>4</sub> .....	4
5. Minimum detectable CH <sub>4</sub> concentration as function of fiber length .....	5
6. Short-range limitation .....	5
7. Long-range limitation .....	5
8. Refractive index as function of molecular weight .....	6
9. Analog response to various gases .....	7
10. Bending losses in fiber at 1,666 nm .....	7

### UNIT OF MEASURE ABBREVIATIONS USED IN THIS REPORT

°C	degree Celsius	μm	micrometer
cm	centimeter	μW	microwatt
dB	decibel	mm	millimeter
dB/km	decibel per kilometer	nm	nanometer
dBm	decibels above 1 milliwatt	nW	nanowatt
g/gmol	gram per gram-mole	pct	percent
h	hour	V	volt
K	Kelvin	vol pct	volume percent
km	kilometer	W	watt

# REMOTE FIBER-OPTIC METHANE MONITOR

By T. H. Dubaniewicz, Jr.,<sup>1</sup> and J. E. Chilton<sup>2</sup>

---

## ABSTRACT

Fiber-optic technology is progressing rapidly, including the development of fiber-optic sensors for many applications. These sensors have the advantages of high sensitivity, light weight, small size, high bandwidth, and freedom from electromagnetic influences. The U.S. Bureau of Mines is investigating the use of fiber-optic technology to monitor mine atmospheres. This report describes a methane monitor based on differential absorption of infrared light. The monitor can detect methane concentrations as low as 0.2 vol pct as far away as 2 km via fiber-optic cable. The upper range is 100 vol pct methane. Since the system requires no electrical power within the mine, it is intrinsically safe.

---

<sup>1</sup>Electrical engineer.

<sup>2</sup>Research chemist.

Pittsburgh Research Center, U.S. Bureau of Mines, Pittsburgh, PA.

## INTRODUCTION

One of the greatest hazards faced by coal miners is the ignition of methane ( $\text{CH}_4$ ) gas.  $\text{CH}_4$  is odorless and explosive when mixed with air to a concentration between 5 and 15 vol pct. Many coal seams naturally liberate  $\text{CH}_4$  into the ventilation air, where it can accumulate to hazardous levels because of ventilation inadequacies or fluctuations. Conventional remote  $\text{CH}_4$  monitors can reliably detect these accumulations. However, these monitors must rely on power supplies that are not intrinsically safe. In case of an emergency, mine electrical power must be shut down. The monitors must then rely on temporary backup batteries. Once these batteries run out, the monitors are disabled, creating a potentially dangerous situation. Modern mining practices have caused special emphasis to be placed on the reliability of  $\text{CH}_4$  monitoring. The depletion of more economical and easily accessible seams has led to the mining of deeper, gassier seams. High-recovery mining methods liberate  $\text{CH}_4$  into the atmosphere more quickly than traditional methods do. These are just a few of the factors that have led to a reported increase in the annual frequency of  $\text{CH}_4$  ignitions by friction in American coal mines (1).<sup>3</sup> A recent survey of 19 reports of investigations on noninjury  $\text{CH}_4$  ignitions involving longwall machines revealed that 4 of the incidents involved improperly operating or calibrated  $\text{CH}_4$  monitors. One way to enhance the reliability of  $\text{CH}_4$  monitoring while eliminating the need for an electrical power supply involves a totally passive, intrinsically safe system that uses fiber optics (FO) to exploit the light-absorbing properties of the gas.

A literature search identified several researchers in other countries such as Japan, England, Norway, and

Australia (2-5) that have made some progress on such a system. Although some researchers reported working models, attempts to obtain units for independent testing were unsuccessful. Since no commercial units were available, an engineering system was developed for research as part of the Bureau's program to improve mine safety. This report focuses on the status of the Bureau's development of a FO  $\text{CH}_4$  monitor.

Over the last several years government and private industry have researched FO sensing, but the mining industry has enjoyed few benefits of that research. Part of the reason is the small return on investment in the limited mining market, but perhaps a bigger reason is the perception that optical fiber is unable to withstand the hostile mine environment. Thousands of miles of fiber placed on the ocean floor for communication systems attest to the strength of FO cable. Fiber is becoming increasingly easier to maintain. For instance, manufacturers recently introduced connectors that require no epoxy or polishing. Cost is becoming another attractive feature as production technology is perfected. The abundance of silica insures the availability of fiber well into the future. Other advantages of fiber include high data capacity and light weight compared with copper cable. Most important, however, are the potential safety benefits of this technology. A well-known characteristic of optical fiber is intrinsic safety. Conventional fiber is made with silica or plastic, or sometimes both (fig. 1). Since these materials are not conductors, sparking is not a problem.

## SYSTEM COMPONENTS

Figure 2 shows the components that comprise the FO  $\text{CH}_4$  monitor assembled by Bureau researchers. A light-beam chopper forms pulses from a tungsten halogen lamp, and a condensing lens focuses the light pulses onto an optical fiber. The fiber then guides the light to the remote site to be monitored. The light exits the fiber, passes through a 50-cm cell where  $\text{CH}_4$  gas may be present, and then enters another fiber that guides the light away from the remote site. A coupler directs the light to two band-pass filters. Detectors behind each filter convert the light into electrical signals that are processed to calculate the concentration of  $\text{CH}_4$  present in the gas cell.

The  $\text{CH}_4$  monitor takes advantage of the optical properties of the gas. Infrared light is absorbed by  $\text{CH}_4$  at two

spectral regions within the optical "window" of conventional silica fiber. One absorption band lies near 1,666 nm and the other lies near 1,330 nm (fig. 3) (2, 6). By observing the amount of light returning to the detector in one of these absorption bands, the concentration of  $\text{CH}_4$  can be determined. The system was designed to monitor light energy near the 1,666-nm peak, primarily because  $\text{CH}_4$

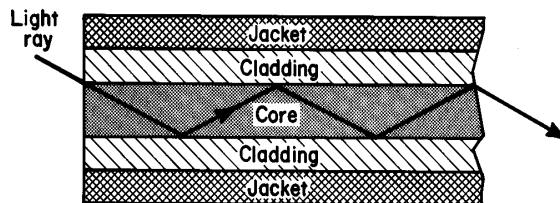


Figure 1.—Profile of fiber-optic cable.

<sup>3</sup>Italic numbers in parentheses refer to items in the list of references at the end of this report.

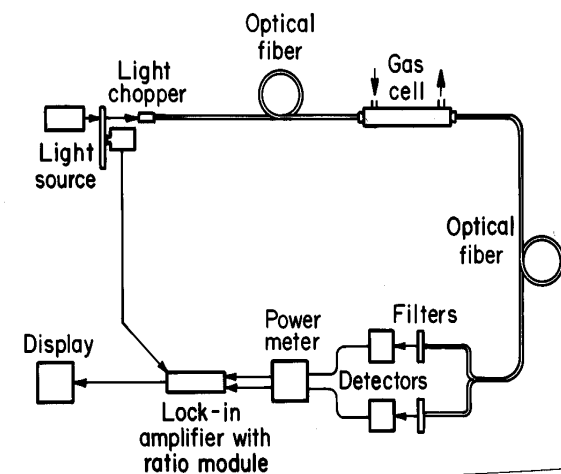


Figure 2.—Fiber-optic CH<sub>4</sub> monitor.

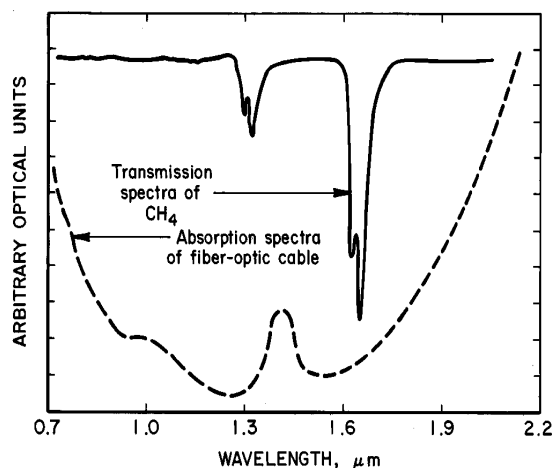


Figure 3.—Fiber-optic window and CH<sub>4</sub> absorption peak.

absorbs much more infrared energy there than at the 1,330-nm peak. A differential detection technique compensates for wavelength-independent fluctuations caused by, for example, lamp dimming or lens dust.

Several types of light sources emit in the 1,666-nm region. One light-emitting diode (LED) met the spectral requirements of the system, but the intensity was marginal. This device had a peak emission wavelength of 1,650 nm, a minimum output power of 100  $\mu$ W, and a maximum spectral width of 190 nm. Although this LED was acceptable for short lengths of fiber, transmission over longer distances required more power. No diode lasers operating at the proper wavelength were commercially available to

test for suitability to the mine environment. Another type of laser that shows promise is the rare-earth-doped fiber laser. These fibers lase when pumped with conventional lasers. Trimming the fiber tunes the output to different wavelengths. These lasers are still in the experimental stage; until more work is done with them, an alternate source must be used.

Tungsten halogen lamps are an inexpensive alternative that emit appreciable amounts of energy in the near-infrared. One of several tungsten halogen lamps evaluated met the requirements of a single-point monitoring system. This was a high-output, miniature lamp with a color temperature of 2,800 K. (The sensor requires infrared energy at a wavelength of 1,666 nm; this wavelength corresponds to a color temperature of approximately 2,200 K.) The lamp coupled more than 400 nW of power in the spectral band of interest through a lens and into a 100- $\mu$ m-diameter fiber core. The life of the 8-W lamp is rated at 3,000 h, equivalent to more than 4 months of continuous use.

Large-diameter silica fibers maximize the amount of light coupled from the lamp filament. Fiber core diameters of up to 1 mm are available, but these are mostly expensive specialty fibers that are generally not available in the lengths required in a mine. The communications industry, which typically uses fiber cores up to 100  $\mu$ m in diameter, strongly influences the cost of fiber. Attenuation also affects the choice of fiber. Although larger core fibers capture more light, they typically exhibit greater attenuation per unit length. Fiber with a core diameter of 100  $\mu$ m and attenuation of 2.5 dB/km (at 1,300 nm) was chosen, considering cost, attenuation, and availability.

In the Bureau's monitor, the CH<sub>4</sub> interacts with the light in a gas cell. The gas cell, constructed in-house, uses 20-power microscope objectives to couple light between the emitting and receiving fiber. This cell had less than 5-dB loss over its 50-cm optical path length. A custom-made field version of the cell based on these results had an attenuation of about 6 dB. This custom-made cell uses a lens tilting alignment technique, eliminating the need for high-precision micropositioners. The simple design greatly eased light coupling while providing ruggedness for the harsh mine environment.

Once the light returns from the remote site, several different approaches can be used to separate the absorption and reference wavelengths from the broad-band beam. One alternative is to split the light and send each beam through a dielectric interference filter. This type of filter is inexpensive, and it passes significantly more light than slit-type spectrophotometers, which is helpful when working with low light levels. A filter with a center wavelength of 1,670 nm and bandwidth of approximately 3 nm was placed in the light path, then tuned to the absorption



wavelength of 1,666 nm by tilting. This tilting technique is useful in compensating for dielectric constructed filters that may be slightly out of specification. An optical power meter using a cooled germanium detector with a noise

equivalent power (NEP) of -80 dBm converted the light to an electrical signal. This signal was processed by a lock-in amplifier and other electronics to indicate the actual CH<sub>4</sub> concentration.

## RESULTS

This assembly of components successfully measured CH<sub>4</sub> below the lower explosive limit. Figure 4 shows the percent absorption for various concentrations of CH<sub>4</sub>. The exponential nature of the graph agrees with the  $1 - e^{(-c/a)}$  response predicted by theory (4), where  $c$  is the concentration of the gas and  $a$  is the constant. The deviation from theoretical values at higher concentrations arises from changes in the refractive index of the analytical system (7).

Figure 5 shows the minimum detectable concentration of CH<sub>4</sub> as a function of fiber length. Two primary factors limit the sensitivity of the monitor. For short lengths of fiber, the sensitivity limit is reached as the fractional change in power caused by CH<sub>4</sub> absorption approaches the NEP of the detector (fig. 6). The horizontal line of figure 5 approximates this limit, calculated as follows:

$$dP = (A)(P_{\max})$$

where  $dP$  = fractional drop in received power when CH<sub>4</sub> is introduced into the cell,

$A$  = fraction of light absorbed by CH<sub>4</sub> in the cell,

and  $P_{\max}$  = power received at the detector for a given length of fiber with no CH<sub>4</sub> present.

Also,  $dP$  = NEP at the limit of detection.

Therefore,  $A = \text{NEP}/P_{\max}$ .

A graph similar to figure 4 can then be used to find the minimum detectable concentration using the calculated value of  $A$ . The actual minimum concentrations measured (about 0.2 vol pct) were slightly higher than the calculated values because drifting of the output signal made it difficult to resolve these small concentrations.

An additional limitation on the sensitivity of the monitor occurs in long lengths of fiber as the maximum power received at the detector approaches the NEP (fig. 7).

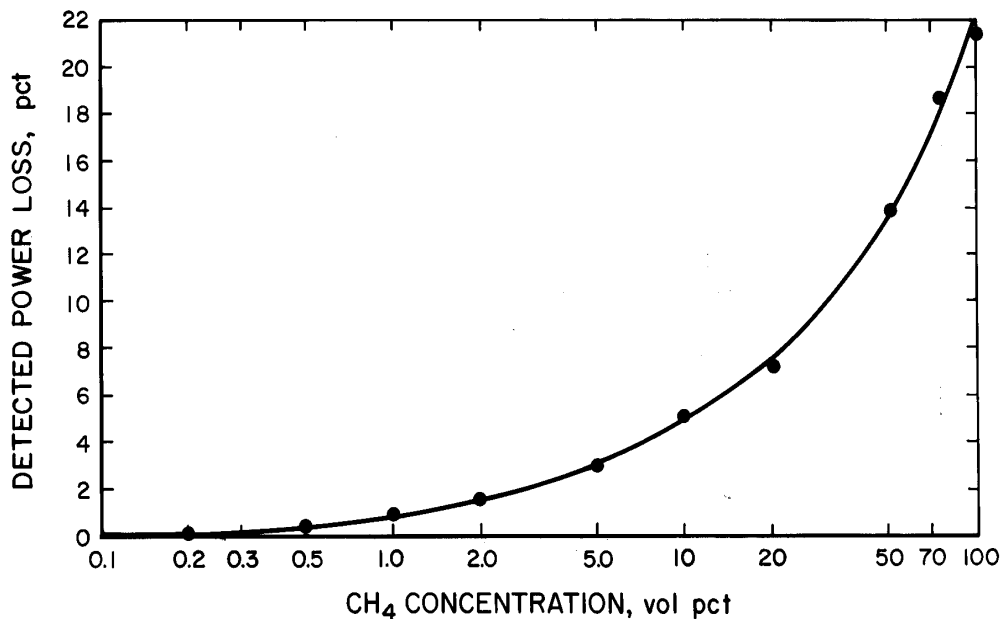


Figure 4.—Percent power loss for various concentrations of CH<sub>4</sub>.

This can be modeled as

$$P_{\max} - dP = \text{NEP},$$

at the detection limit.

Therefore,  $A = (P_{\max} - \text{NEP})/P_{\max}$

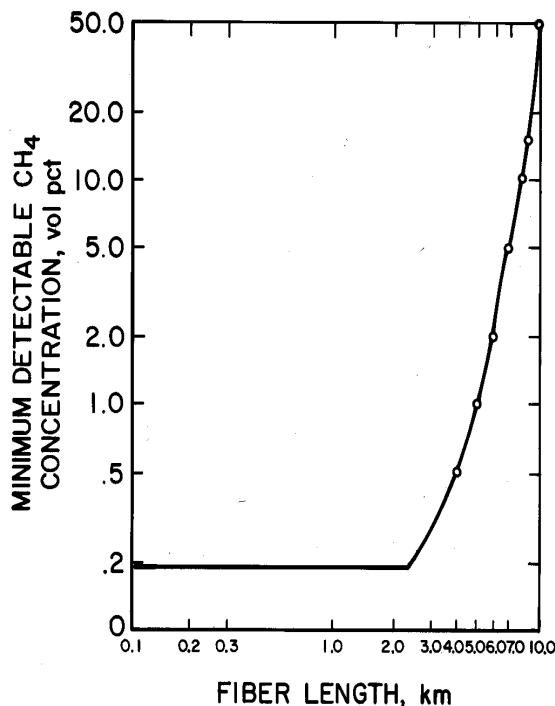


Figure 5.—Minimum detectable  $\text{CH}_4$  concentration as function of fiber length.

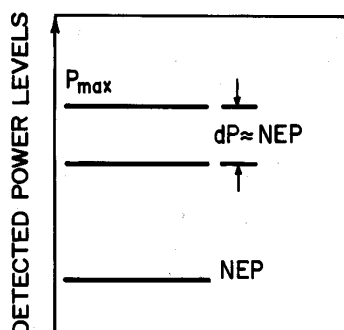


Figure 6.—Short-range limitation. (NEP = noise equivalent power of detector;  $dP$  = fractional drop in received power when  $\text{CH}_4$  is introduced into gas cell;  $P_{\max}$  = power received at detector for a given length of fiber with no  $\text{CH}_4$  present.)

Again, this calculated  $A$  is used to find the minimum detectable concentration from a graph similar to figure 4. This effect is responsible for the sharp upturn in figure 5 after 2 km.

Modifying different components of the sensor affects the performance curve of figure 5. To increase the sensitivity in the short range, one can increase the path length of the gas cell or use a narrower filter. This would shift the horizontal portion of the curve downward. These changes also would tend to decrease the optical efficiency of the sensor, shifting the vertical portion of the graph to the left. Alternatively, increasing the light power or using a detector with a lower NEP would greatly improve performance in the long range while providing moderate improvement in the short range.

### TEMPERATURE EFFECTS

During a series of in-mine tests, changes in environmental temperature caused a noticeable drift in the output of the monitor. For example, an  $8^\circ \text{C}$  change in ambient temperature caused the output to drift by 3 pct  $\text{CH}_4$ . Other researchers have noted these effects and have attributed them to temperature-sensitive optical filters (4). Based on these results, the system will require temperature stabilization. A parallel fiber with a reference gas cell can be added to the system and monitored to compensate for subsequent temperature-induced errors.

### REFRACTIVE INDEX EFFECTS

Other hydrocarbons similar in molecular structure to  $\text{CH}_4$  were introduced into the gas cell to investigate their effect on the monitor. The response to ethane ( $\text{C}_2\text{H}_6$ ) was about one-third of the response to  $\text{CH}_4$ . The introduction

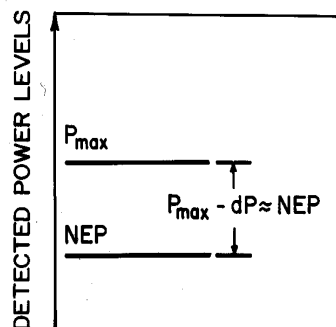


Figure 7.—Long-range limitation. (NEP = noise equivalent power of detector;  $dP$  = fractional drop in received power when  $\text{CH}_4$  is introduced into gas cell;  $P_{\max}$  = power received at detector for a given length of fiber with no  $\text{CH}_4$  present.)

of propane ( $C_3H_8$ ) and butane ( $C_4H_{10}$ ) into the gas cell caused unexpected negative readings. The index of refraction of the gases is the likely cause of these errors.

Whenever light passes through any system of glass lenses (refractive index of 1.53) to air (refractive index of 1.000292), part of the light reflects and the rest passes through. For a single air-glass interface, Fresnel's expression gives the reflected light  $R$  as follows:

$$R = (b - n)^2 / (b + n)^2,$$

where  $b$  is the refractive index of glass (a constant), and  $n$  is the refractive index of the gas. The value of  $n$  varies from 1.000292 for air to 1.001410 for  $C_4H_{10}$ . By substituting the factor  $g$  for  $n - 1$ , the equation can be rewritten as follows:

$$R = (b - 1 - g)^2 / (b + 1 + g)^2.$$

By differentiating  $R$  with respect to the variable  $g$ ,

$$dR = -4b(b - 1 - g) / (b + 1 + g)^3 dg,$$

which for  $g < 1$  approximates to

$$dR = -0.20 dg.$$

The reflected light  $R = (I_o - I) / I_o$ , where  $I_o$  is the initial intensity and  $I$  is the transmitted intensity of light.

Then 
$$dR = -dI / I_o.$$

And finally, 
$$dI = 0.20 I_o dg.$$

This expression states that the increase in transmitted light is proportional to the increase in gas refractive index. This calculation is for a single surface, but similar expressions hold for multiple lens-air interfaces as well. The function  $f = (n - 1) \times 10^6$ , where  $n$  is the refractive index of the gas, is plotted in figure 8 versus molecular weight. The data for  $H_2$  and hydrocarbons from  $CH_4$  through pentane ( $C_5H_{12}$ ) fall on a straight line when plotted against the molecular weights. Reference 8 provided the refractive index values taken at the Na D line wavelength. The refractive indexes for  $C_3H_8$  and  $C_4H_{10}$  were estimated from this graph from the intersection of their molecular weights and the hydrocarbon function line.

When pure gases were fed into the gas cell, channel "a" of the optical power meter measured light energy from the cell at the 1,666-nm wavelength and channel "b" measured light energy at the reference wavelength. Both channels were input to a lock-in amplifier. The ratio of the two

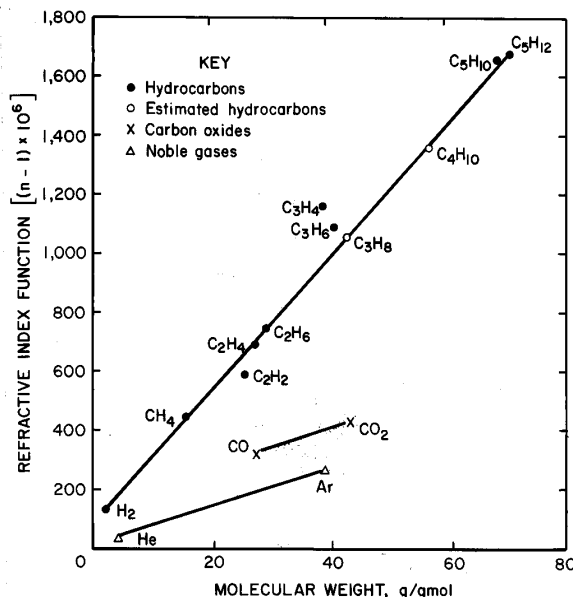


Figure 8.—Refractive index as function of molecular weight.

amplified signals was then displayed as a voltage. This displayed voltage was initially set to 10.00 V with  $N_2$  gas in the cell. Several gases caused a change in the voltage, and figure 9 shows the function of  $(10 - V)$  versus the refractive index of the gases. This figure shows that  $CH_4$  and  $C_2H_6$  are positive and to the right of the general curve, because both gases absorb light. Both  $C_3H_8$  and  $C_4H_{10}$  have negative values, indicating an increase of light energy. This increase can only occur when the refractive index change allows more light to pass through the gas cell. In this plot, even He acts as if there were an absorption of energy at 1,666 nm. Since He lacks absorption lines in this portion of the spectrum, again the refractive index effect is indicated. The result is that gases with significantly different indexes of refraction than air have a wavelength-dependent effect on the transmission of light through a system of lenses, and such gases interfere with the measurement of  $CH_4$  in the gas cell. For instance, the monitor's response to equal quantities of  $C_4H_{10}$  and  $CH_4$  would almost cancel each other, resulting in a null reading. Modifying the system to monitor a reference wavelength very close to the absorption band will minimize this wavelength-dependent error. Any changes associated with this refractive index effect will be nearly the same in both the reference wavelength and the absorption wavelength, and will cancel when the ratio is determined.

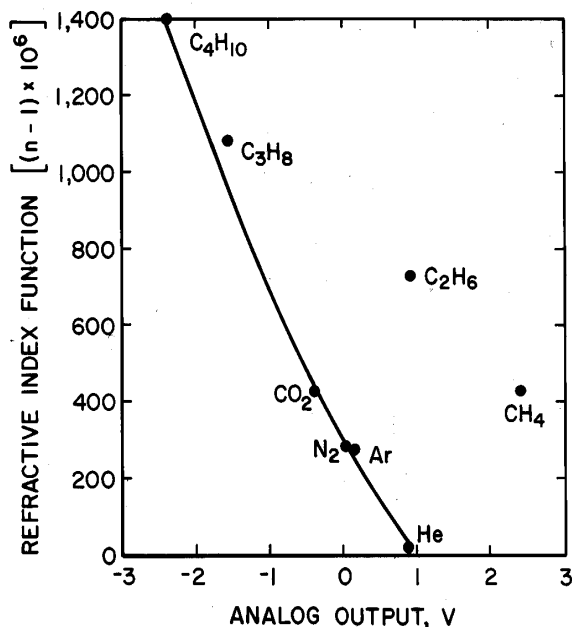


Figure 9.—Analog response to various gases.

#### MACROBENDING<sup>4</sup> EFFECTS

Light losses from macrobends in the fiber are significant in the 1,666-nm region (6). Macrobend losses in silica fiber become apparent around 1,500 nm, and the losses increase with wavelength. As a result, the output of the monitor drifted as the fiber was bent excessively. A significant portion of the total power also was lost as the fiber was bent. Light losses of 20 pct occurred when 100- $\mu$ m-core-diameter fiber contained in a 3-mm-diameter

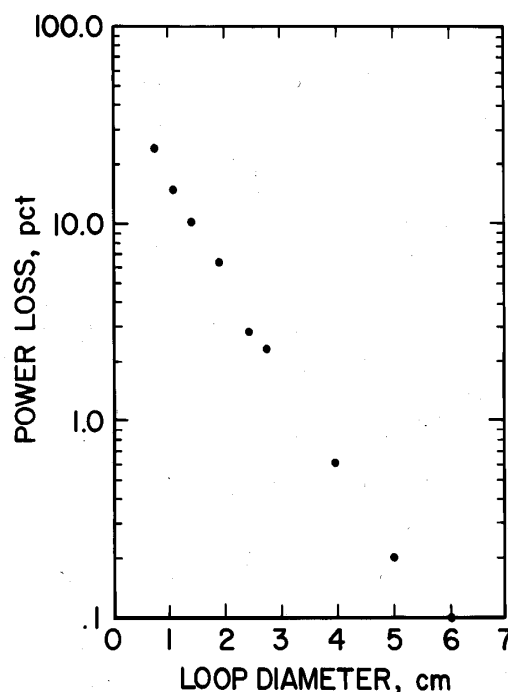


Figure 10.—Bending losses in fiber at 1,666 nm.

jacket was looped around a 1-cm dowel. Losses decreased to less than 0.1 pct for loop diameters greater than 6 cm (fig. 10). Again, choosing a reference wavelength within a few nanometers of the absorption line will minimize the errors caused by wavelength-dependent losses such as this. However, excessive bending must be avoided to maintain an acceptable signal-to-noise ratio.

#### SUMMARY

A FO-based remote CH<sub>4</sub> monitor was assembled and tested by Bureau researchers. The system detects CH<sub>4</sub> by measuring the absorption of near-infrared light as it passes through the gas. The FO cable used to direct the light to and from the remote site is intrinsically safe and therefore, eliminates the sparking hazard found in the power supply of electrically based remote monitors. This monitor can detect CH<sub>4</sub> concentrations as low as 0.2 vol pct as far away as 2 km. The upper range is 100 vol pct CH<sub>4</sub>.

These results are encouraging; however, this system requires more work before it is ready for mine usage.

Temperature-, bending-, and refractive-index-induced errors must be decreased. Temperature stabilization will be required to reduce the temperature-induced error to an acceptable level. Choosing a reference wavelength close to the absorption line will help to minimize the errors associated with wavelength-dependent errors seen with the bending and refractive index effects. Furthermore, some method of monitoring multiple sites is needed to make the system economical. The tungsten lamp provided enough power for a single-point sensor; however, a more powerful light source is required to overcome the losses of multiple gas cells.

<sup>4</sup>Macrobending refers to bending the fiber into loops with a diameter much larger than the fiber diameter.

## REFERENCES

1. Watson, R. W. Prevention of Friction Ignition on Longwall Sections. *J. Mines, Met., and Fuels*, June-July 1989, pp. 261-265.
2. Chan, K., H. Ito, and H. Inaba. All-Optical-Fiber-Based Remote Sensing System for Near Infrared Absorption of Low Level  $\text{CH}_4$  Gas. *J. Lightwave Technol.*, v. LT-5, No. 12, Dec. 1987, pp. 1706-1711.
3. Hordvik, A., A. Berg, and D. Thingbo. A Fiber Optic Gas Detection System. Paper in Proceedings of 9th European Conference on Optical Communication (Geneva, Oct. 23-26, 1983). North-Holland, Amsterdam, 1983, pp. 317-320.
4. Dakin, J. P., C. A. Wade, D. Pinchbeck, and J. S. Wykes. A Novel Optical Fibre Methane Sensor. *Proc. Soc. Photo-Opt. Instrum. Eng.*, v. 734, 1987, pp. 254-260.
5. Hopkins, J. C., P. J. Samson, and A. D. Stuart. A Fibre Optic Based Continuous Mine Monitoring System. Paper in Proceedings of the 7th International Conference on Optical Fibre Sensors (Sydney, Aust., Dec. 2-6, 1990). *Inst. Radio and Electron. Eng.*, 1990, pp. 207-210.
6. Kalish, D., and L. G. Cohen. Single Mode Fiber: From Research and Development to Manufacturing. *AT&T Tech. J.*, v. 66, No. 1, Jan.-Feb. 1987, pp. 19-32.
7. Willard, H. H., L. L. Merritt, Jr., J. A. Dean, and F. A. Settle, Jr. *Instrumental Methods of Analysis*. Wadsworth, 7th ed., 1988, pp. 159-163.
8. Weast, R. C. (ed.). *Handbook of Chemistry and Physics*. Chem. Rubber Publ. Co., 54th ed., 1974, p. E-224.